Journal of Building Engineering xxx (xxxx) 103049

Contents lists available at ScienceDirect

Journal of Building Engineering

journal homepage: www.elsevier.com/locate/jobe

Long-term performance of galvanic anodes for the protection of steel reinforced concrete structures

Deepak K. Kamde [a, *], Karthikeyan Manickam [a], Radhakrishna G. Pillai [a], George Sergi [b]

[a] Department of Civil Engineering, Indian Institute of Technology Madras, Chennai, India
[b] Vector Corrosion Technologies, Cradley Heath, United Kingdom

ARTICLE INFO

Keywords:
Concrete
Steel
Chloride
Corrosion
Repair
Galvanic anodes
Cathodic protection

ABSTRACT

Corrosion is one of the major deterioration mechanisms of reinforced concrete structures. The conventional patch repair without addressing the root cause of the corrosion can lead to repeated repairs. Therefore, a form of cathodic protection (CP) using galvanic anodes is a viable electrochemical technique to mitigate corrosion. However, practitioners hesitate to adopt CP for repair due to the lack of evidence and limited knowledge on the long-term performance of galvanic anodes in concrete systems. For this, two reinforced concrete panels with and without discrete galvanic anodes were cast with admixed chlorides and exposed to a natural environment for 12 years. Electrochemical measurements, such as depolarized corrosion potentials and corrosion rate of the rebars, and output protection current density of the galvanic anodes were measured. In addition, physico-chemical characteristics such as elemental composition, residual lithium content, pH, pore volume, and pore size distribution in the encapsulating mortar were determined on a 12-year in-service galvanic anode. This paper indicates that the alkali-activated galvanic anodes can protect the steel rebars from corrosion for at least 12 years. Analysis after 12 years showed that the pores in encapsulating mortar were partially filled with zinc corrosion products, resulting in substantial pore blockage surrounding the zinc metal. This led to a reduction in the pH buffer in the vicinity of the zinc metal. Also, characteristics of tie wire-zinc metal interface may affect the long-term performance of galvanic anodes. Based on this study, specifications are proposed to help manufacturers to design durable galvanic anode systems.

List of symbols and abbreviations

%bwob	% by weight of binder
CP	Cathodic protection
dcritical	Critical pore size
MIP	Mercury Intrusion Porosimetry
RC	Reinforced concrete
RR	Reference region
SCE	Saturated calomel reference electrode
EDX	Energy Dispersive X-ray Analysis

1. Introduction

Worldwide, many reinforced concrete (RC) structures were built for a design service life of about 50 years (designed by old standards). Most of them are facing distress due to corrosion of reinforcement. Protection of these structures is utmost important. The emphasis on protection of these structures varies across the globe depending on the period of major economic developments. In addition, many nations in the past two decades have built many RC infrastructure systems such as railways, highways, buildings, and ports for a desired service life of 100 years. Many of them are located in a chloride-rich environment. To achieve such long service life, RC systems (concrete and steel) should have adequate corrosion resistance. However, due to accelerated construction, much of the infrastructure are built without the quest for quality of construction practices and materials, which can result in premature corrosion [1–4]. NACE Impact Report states that about 50% of structures require major repair within ten years after construction [5]. This leads to a huge construction budget to refurbishment and repair of existing structures [6]. Generally, conventional repairs, such as patchwork using complete or partial replacement of concrete/mortars, are adopted to repair RC systems. The patch repairs alone do not address the root

* Corresponding author.
E-mail address: deepak.kamde89@gmail.com (D.K. Kamde).

https://doi.org/10.1016/j.jobe.2021.103049
Received 20 May 2021; Received in revised form 28 July 2021; Accepted 29 July 2021

cause of corrosion and create the difference in the electrochemical characteristics of steel rebar in parent and repair concrete, leading to premature failure of repair and need for repeated repair. The repeated repairs can be eliminated by the use of cathodic protection (CP) systems using galvanic anodes in the critical locations. Critical locations can be identified by detecting locations where corrosion is already initiated and by estimating residual service life of structural elements where corrosion is not yet initiated, but may initiate within a few years (say, less than 10 years). However, very few structures are provided with CP systems to repair the RC systems. For example, in India, only about 70 structures were repaired using galvanic anodes until 2020 [7]. The practitioners are hesitant to use the galvanic anodes due to (i) the limited availability of evidence of the long-term performance of galvanic anode systems in RC structures, (ii) limited knowledge on corrosion characteristics of galvanic anodes in-service, and (iii) unavailability of standards or guidelines in developing nations to select and use the galvanic anodes, which are the focuses of this paper.

The remainder of the paper is organized in the following manner: first, the difference between repair of full structures with and without galvanic anodes is discussed. Then, a literature review on long-term performance and the factors affecting the long-term performance of galvanic anodes is discussed. After that, an experimental program to evaluate the long-term performance of galvanic anodes is discussed. The results from the long-term electrochemical assessment and the effect of physico-chemical characteristics of galvanic anodes on their performance are presented. Based on the results, a list of specifications is proposed to facilitate and ensure the long-term performance of galvanic anodes. Finally, conclusions from this research are presented.

1.1. Repair of reinforced concrete systems

Fig. 1 shows the difference in the patch repair without and with galvanic anodes. If patch repair is employed without galvanic anodes (PR strategy), the following consequences can occur (see Fig. 1(a)):

(i) **Incipient Anode effect, sometimes referred to as the Halo or Ring effect**: Following repair, the rebar in parent and repair concrete is exposed to different physical (relative humidity, voids, cracks, etc.) and chemical (chloride concentration, pH, etc.) conditions. Prior to repair, steel adjacent to the corroding steel is receiving a level of cathodic protection by the corroding (anodic) region. After repair, this fortuitous local protection is removed so that the above mentioned variation in properties between parent concrete and repair material create an electrochemical potential difference on the rebar surface stretching across the interface of parent and repair concrete [8,9] — leading to the formation of a corrosion cell and accelerated corrosion around the perimeter of the patch repair [9,10].

(ii) **Residual chloride effect**: The rebar in the repaired region, especially if the parent concrete surrounding the steel is not totally removed, may continue corroding due to residual chlorides on the steel rebar surface [7]. This can continue the reduction of the cross-sectional area of rebar even after the repair.

(iii) **Hidden/upcoming corrosion**: This concerns the rebar in the parent concrete which was not addressed at the time of repair either because there was no sign of corrosion or the electrochemical measurements indicated no corrosion activity. However, in a matter of a few months or years; new, and existing chlorides in the concrete will further diffuse into the concrete and initiate the corrosion of steel located in non-patched parts of the structure. This will lead to corrosion of the rebars in locations where repair was not carried out in the earlier intervention.

As a result, these repair strategies can fail within about five years [6,7,11]. Soon, a large number of structures may undergo repeated repair — resulting in a large number of accumulation of structures for re-

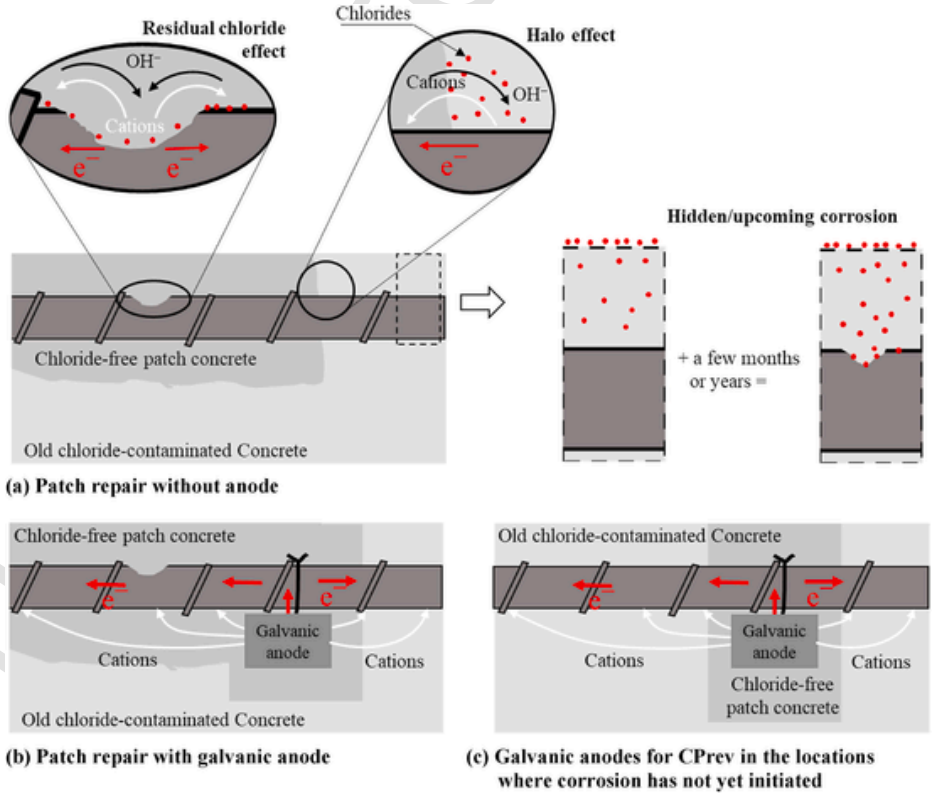

Fig. 1. Schematic of the patch repair without and with CP using galvanic anodes. (a) Patch repair without anode. (b) Patch repair with galvanic anode. (c) Galvanic anodes for CPrev in the locations where corrosion has not yet initiated.

pair [9,12]. Therefore, there is a dire need to adopt a suitable repair strategy, which can arrest the corrosion due to Incipient Anode effect, sometimes referred to as the Halo or Ring effect, residual chloride effect, and hidden/upcoming corrosion.

Fig. 1(b) shows how the repair using galvanic anodes can eliminate such effects and help to facilitate a durable repair life [13]. Here, the anode is more electrochemically negative (say −1100 mV) than the steel rebar (say −350 mV). They are electrically connected using tie wires to the rebar and concrete act as the ionic conductor [14]. The potential difference across the galvanic anode and rebar is more than the potential difference between two points on steel rebar at the repaired or parent concrete, or interface of parent and repair concrete [15]. Therefore, the metal in galvanic anode preferentially corrodes to protect the rebars up to the throwing distance until the galvanic anode is consumed. The throwing distance is the area or sphere of influence surrounding the galvanic anode up to which it can protect the rebars from corrosion. The throwing power depends on various factors such as type of anode used, resistivity of concrete, rate of corrosion of steels, relative humidity of concrete, etc. [16,17]. Therefore, the design of CP systems using galvanic anode (numbers and location) is case-specific and is decided based on throwing power of the galvanic anodes [18]. To address hidden or upcoming corrosion, estimating the residual service life of structural element can help in deciding if the structural element needs immediate attention or can be addressed later. If residual service life is less than 10 years, then installation of galvanic anodes in these locations can delay the initiation of corrosion (see Fig. 1(c)). If repair of structure is adequately planned by installation and replacement of galvanic anodes, it is reported that the level of civil infrastructure needing repair can be decreased by 2–5 times [8,19]. The performance of galvanic anodes depends on various factors, which are discussed later in this paper.

1.2. Performance assessment of galvanic anodes in reinforced concrete systems

Conventionally, the performance of galvanic anode CP systems in concrete is assessed based on the '100 mV potential shift' of the steel over a period of 24 h as per ISO EN 12696 [20]. For this, the following measurements are required:

(i) **instant-off potential ($E_{i\text{-}Off}$)**: the potential of steel rebars with respect to reference electrode measured within 1 s of disconnecting the anode from the steel rebars
(ii) **24-h depolarized potential ($E_{24\text{-}h}$)**: the potential of steel rebars with respect to a reference electrode after the anodes are disconnected for 24 h.

As per ISO EN 12696, the difference between $E_{i\text{-}Off}$ and $E_{24\text{-}h}$ should be greater than 100 mV [20]. For this, monitoring box is required to be installed at specific locations on the structures, which is mostly not practiced or not maintained for a long time, which has hindered their long-term performance evaluation [7]. Much of the literature reports that galvanic anode CP systems are primarily designed to offer corrosion prevention, i.e. prevent initiation of corrosion, and cannot achieve 24 h depolarization of 100 mV [21,22]. Therefore, instead of '100 mV potential shift' criterion, the measurement of depolarized potential or the rate of corrosion of the steel in a depolarized state is adopted in this study. This can provide true corrosion conditions of steel rebar surfaces [19].

1.3. Factors affecting the long-term performance of galvanic anodes in concrete systems

Fig. 2 shows a schematic of typical alkali-activated discrete galvanic anodes with three important elements: (i) galvanic metal, (ii) encapsulating mortar, and (iii) tie wires. The shape and size of anodes vary with manufacturers and the purpose of use. Galvanic metal corrodes to protect the reinforcement and is selected such that it is more electronegative than steel rebars. Commonly used galvanic metals are magnesium, aluminum, zinc, or their alloys [9]. To keep the galvanic metal active for corrosion, the galvanic metals are embedded in specially formulated encapsulating mortar [8]. The activating agent in the encapsulating mortar, however, should not aggravate the corrosion of steel rebars [23]. Details on the required characteristics of encapsulating mortar are discussed later.

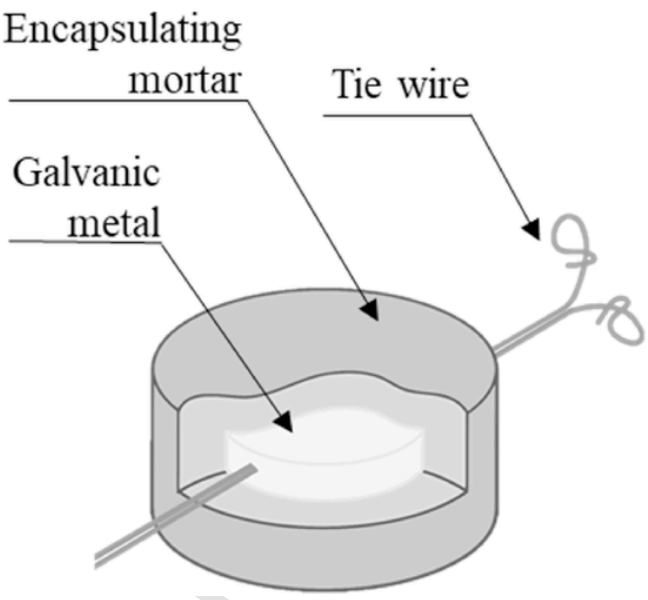

Fig. 2. Schematic of typical alkali-activated discrete galvanic anode.

Many literature worldwide (from Netherlands, England, USA, Canada, India, and Venezuela) report that the good quality galvanic anodes can perform for a service life of 10–25 years [7,19,24–26]. The performance of galvanic anodes depends on various factors, such as resistivity of old and repair concrete, relative humidity of concrete, and steel density to be protected, pH, and porosity of encapsulating mortar, relative humidity at the interface of a galvanic metal and encapsulating mortar. The factors such as steel density, the relative humidity of concrete, and resistivity of concrete are well reported in the literature [15]. Many of these factors can be accommodated by adopting adequate design. However, there are a few factors such as pore volume, pH of encapsulating mortar and effect of alteration of encapsulating mortar characteristics during service, which can influence the performance of galvanic anodes [27,28] are discussed later.

1.3.1. Activators and humectants

The continuous and long-term corrosion of zinc can be achieved by using adequate encapsulating mortar with (i) activators and (ii) humectants [29,30]. Activators increase the dissolution kinetics of anodes and maintain a high corrosive environment around the zinc metal [31] and are classified into two types: (i) halide and (ii) alkali activators [14,32]. Halide activators such as fluoride, chloride, bromide, iodide act as catalysts to maintain a continuous corrosive environment around the anode metal. As the zinc corrodes, the soluble corrosion products migrate through encapsulating mortar, aiding the continuous corrosion of the metal [33]. However, they may lead to corrosion of steel rebars due to the diffusion of the halide anions towards the steel surface, especially when the anodes are placed close to the rebar [23]. On the other hand, alkali activators, such as lithium hydroxide, sodium hydroxide, potassium hydroxide, help in maintaining the pH of the encapsulating mortar to more than 14, thereby, keeping the zinc active [23,34,35]. During this process, these activators get consumed and can lead to the reduc-

tion of pH at galvanic metal-encapsulating mortar. For example: zinc oxidises by loosing its two electrons and reacts with an equivalent amount of OH–, which has to be supplied by the activator, and is a service life determining factor (as is mass of zinc) (see Equations (1) and (3)).

$$Zn \rightarrow Zn^{2+} + 2e^{-} \quad (1)$$

$$Zn^{2+} + 4OH^{-} \rightarrow Zn(OH)_4^{2-} \quad (2)$$

$$Zn(OH)_4^{2-} \rightarrow ZnO + 2OH^{-} + H_2O \quad (3)$$

Zinc reacts with both acids and bases to form salt. However, the rate of corrosion of zinc is high at pH less than 6 (acidic) and greater than 12.5 (basic) [36]. The rate of corrosion of Zn is relatively low for pH between 6 and 12.5 [27], which can also be termed as passivation of zinc". Therefore, maintaining high alkalinity in encapsulating mortar of alkali-activated mortar is essential. It was reported that the activity of zinc can be enhanced by adding either 170 g KOH/100g of zinc or by 73 g LiOH/100g of zinc [8,27]. In another investigation, it was reported that the concentration of LiOH was significantly reduced in the encapsulating mortar after about 14 years of service — leading to a decrease in pH from a designed value of 14.6 to 13.8 [19]. However, these anodes were intended to achieve repair life of 10 years, which was designed by providing sufficient zinc and lithium hydroxide content in the encapsulating mortar. This reduction in pH can result in the reduced effectiveness (say, output current, throwing distance, etc.) of the galvanic anode [19], which is why the amount of added alkali to the activating mortar should be determined before production so that the desired service life is achieved.

Humectants are hygroscopic materials, which maintain adequate humidity around the anode metal for continuous corrosion of the galvanic metal. They also reduce the build-up of ions at the metal surface to facilitate ionic conduction by allowing them to diffuse (a slow process) into the surrounding moist pore structure [24,29,30]. A few commonly used humectants are lithium bromide, lithium nitrate, calcium chloride, etc. During the process of ionic conduction and electrochemical reactions, the concrete in the vicinity of steel will be enriched with ions such as OH^-, Li^+, Na^+, and K^+. The region around the anode will be enriched with chlorides and other anions due to the diffusion or migration of ions from chloride contaminated concrete [37], and may affect the performance of the galvanic anode.

1.3.2. Characteristics of encapsulating mortar

The pore structure of the encapsulating mortar provides space for accommodating the zinc corrosion products and interconnected pores provide the path for movement of zinc corrosion products [8]. It was reported that the pore volume of 16–23% performed best [24,38]. Another research by Schwarz et al. (2016) reported that the encapsulating mortar with volumetric porosity of more than 35% can help to provide a path for movement of zinc corrosion products away from the anode – making fresh zinc surface available for corrosion [27]. Encapsulating mortar with low pore volume can result in clogging of pores with corrosion products and hinder the movement of corrosion products and reduce the ionic transport through the encapsulating mortar [38,39]. Therefore, the pore structure of encapsulating mortar should be designed such that it diffuses the corrosion products away from the zinc metal to make unreacted zinc available for corrosion. The investigation on various pore volume is out of scope of this paper. In addition to pore volume, pH of encapsulating more plays an important role. An advantage of highly alkaline encapsulating mortar (pH > 14) is that the zinc corrosion products exist as soluble zincate ions, which can migrate through the pores away from the zinc-mortar interface and maintain clear pathways for current flow for longer period [19]. The authors could not find literature on evaluating the effects of the reduction of porosity of encapsulating mortar on the long-term performance of anodes, which is one of the focuses of this paper.

2. Research significance

As detailed in Section 1.1, conventional patch repairs can result in repeated repairs of adjacent regions. The National Association of Corrosion Engineers IMPACT report states that nearly 4% of worldwide GDP is spent to control corrosion of infrastructure [5], most of which is spent to repair the concrete systems. The adequate implementation of CP using galvanic anodes for full structure as CP and CPrev can reduce the frequency of repair and cost of corrosion. The results presented in this paper show that suitable galvanic anodes can protect RC systems for more than 12 years. It is hoped that this will encourage practitioners to incorporate galvanic anodes in the repaired areas of RC systems to significantly prolong their performance. The specifications proposed in this paper can help to design durable galvanic anode systems.

3. Experimental methods

The experimental program is designed in two phases, Phase I: long-term performance of galvanic anodes and Phase II: Physico-chemical characterization of a 12-year-old galvanic anode, which is aiming to identify factors affecting the long-term performance of galvanic anodes.

3.1. Phase I: Long-term performance of galvanic anodes

3.1.1. Specimen preparation and exposure condition

Fig. 3(a) shows the schematic of the panels with a dimension of 1 × 1 × 0.25 m. For this, 32 mm diameter rebars were cut to a length of 1.05 m. The rebars were placed 100 mm apart and electrically disconnected to each other (Fig. 3(b)). A total of 18 rebars, 9 top and 9 bottom rebars, were placed so that the top set of rebars were ≈85 mm away from the bottom set. The steel to concrete surface area ratio was 1. For this, only top and bottom surface area of concrete panel were considered. The top face of the panel will augment to the severe exposure condition by ingress of moisture and oxygen to the steel rebars, whereas, bottom face of panel will only be provide the access of oxygen, but not moisture. Side faces were not considered because the extent of ingress of moisture and oxygen from sides will be limited to a few mm from either side face of the panel. Two panels (i) with and (ii) without galvanic anodes were cast. To simulate the condition of existing structures with chlorides in concrete, the concrete in both panels was premixed with 2% chloride by weight of cement (%bwoc). Panel 1 was divided into three parts considering the type of anode installed. The part of Panel 1 with Anode A1, A2, and A3 is labeled as Part A1, A2, and A3, respectively [see Panel 1 in Fig. 3(b)]. The rebars in Panel 1 were connected using three numbers of three types of anodes, labeled A1, A2, and A3 (a total of 9 anodes). The anodes were tied to rebars with a c/c distance of 400 mm (see Fig. 3(a)). Note that the anodes were electrically disconnected. The difference between anodes A1, A2, and A3 is the surface area of the metal piece. The surface area of metal pieces in A1, A2, and A3 were × 1, × 2, and × 4 the surface area of Anode A1, respectively (see Fig. 3(b)). The weight of anode metal in Anode A1, A2, and A3 were × 1, × 2, and × 4 the weight of Anode A1, respectively. The weight (gm) to surface area of anode metal (cm^2) for all anodes was 1.65. All the rebars and anodes were connected together outside the panel system using electric wire and junction box, which allowed the measurement of the depolarized potential of the steel 24 h after disconnection of the anodes and the corrosion rate of the steel rebars without the influence of the anodes. Panel 2 was prepared as a control specimen with no anodes. Table 1 shows the mix proportions of concrete used to cast both slabs. After casting, both the panels were cured with wet sack for 7 days and were exposed to a natural environment within 2 km from the seashore of a coastal city in western India for 12 years. The panels experienced an average of 4 months per year of heavy rain and an environment with relative humidity ranging from 55 to 80% for the re-

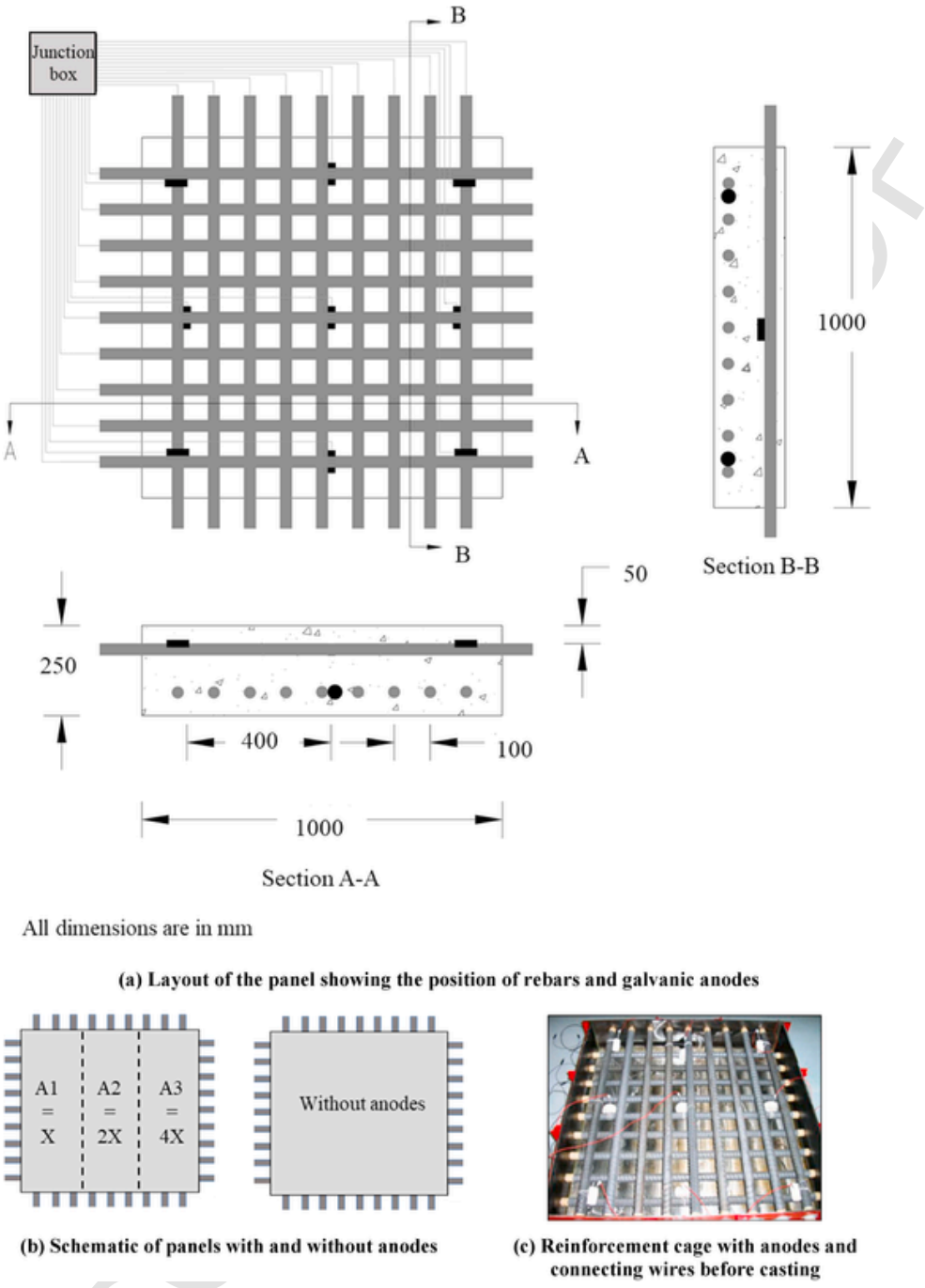

Fig. 3. Panels schematic and photograph for assessing long-term performance of galvanic anodes (X is the surface area of metal in Anode A1). (a) Layout of the panel showing the position of rebars and galvanic anodes (b) Schematic of panels with and without anodes (c) Reinforcement cage with anodes and connecting wires before casting.

Table 1
Mix proportion of concrete used to cast slabs.

Material	Quantity (kg/m^3)
Ordinary Portland Cement	360
20 mm aggregate	683
10 mm aggregate	455
Fine aggregate	612
Water	198
NaCl	11.9

maining of each year and temperature ranging from ≈15 to ≈35 °C throughout the year [40]. This created a highly corrosive environment for the RC panels.

3.1.2. Electrochemical measurements

The output protection currents from anodes were measured every month for the first seven months of exposure after casting. Then, the panels were left to natural exposure for about eight years. During this time, the measurements were not recorded. Then, output protection current from the anodes and 24-h depolarized potentials ($E_{24\text{-}h}$) of steel rebars were measured every six months for about four years. Fig. 4 shows the schematic demonstrating the procedure to measure the out-

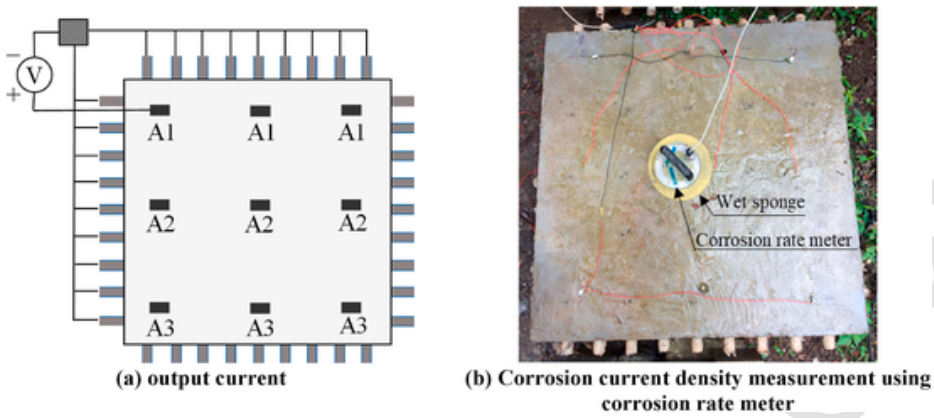

Fig. 4. Measurement of output current and corrosion current density. (a) Output current (b) Corrosion current density measurement using corrosion rate meter.

put current from each type of anode. For this, 1 Ω resistor was connected in series between the anodes of each type and all the rebars. A 5.5 digit multimeter was used to measure the potential difference across the 1 Ω resistor. Measured potential difference across the resistor was used to calculate the current using Ohm's law. To measure the depolarized potential, the anodes were disconnected from the rebars for 24 h. Then, the potential of each rebar was measured using a saturated calomel reference electrode (SCE) positioned on the surface of the concrete directly above the measured steel rebar.

In addition, corrosion rates of depolarized steels were measured at the end of 12 years of exposure using a corrosion rate meter (see Fig. 4 (b)). For this, a commercially available corrosion rate meter was used. The working principle of the corrosion rate meter is scientifically validated and presented by Andrade and others in Refs. [41–43]. In the sensor of the corrosion rate meter, the following electrodes were present: reference electrode (RE) 1, counter electrode, RE 2, RE 3, and guard ring electrode. During measurements, the sensor was placed on the saturated concrete surface such that RE 1, 2, and 3 were aligned in the direction of the steel rebar. Each steel rebar was isolated from other steel rebars and externally connected to the sensor while corrosion current density was measured. For adequate ionic conductivity, a wet sponge was placed in between the sensor and the concrete surface. The potential difference between the RE 2 and 3 were measured. The small potential shift (DE) is applied between steel rebar and counter-electrode, which alters the potential difference between two electrodes. Then, a current (I_{CE}) is applied from the guard ring until the potential between two electrode returns to the original value. The current is flowing between the counter electrode and working electrode in the concentrated region (i.e., confined steel surface area). Using the applied potential, measured current, and Equation (1), resistance to polarization (Rp) is determined by subtracting the ohmic drop across concrete (R_{Ω}) [44].

$$Rp = \left(\left(\frac{\Delta E}{I_{CE}}\right) - R_{\Omega}\right) \times Confined\ steel\ surface\ area \tag{4}$$

It was reported that the measured rate of corrosion in this way is only correct over a range of half to double the recorded level [41–43]. On the other hand, a few authors reported that the calculation of corrosion rate from the corrosion rate meter is not accurate because the Stern-Geary equation is not applicable for the localized corrosion, which normally occurs in RC systems [45]. Therefore, it may not allow an accurate calculation of the rate of corrosion [46,47]. However, here, as the geometry of the slab samples is uniform. Therefore, corrosion rate measurements on individual rebars can be compared.

3.2. Phase II: Physico-chemical characterization of a 12-year-old galvanic anode

A cylindrical concrete core containing one of the embedded anodes of Type A1 was extracted from Panel 1 (see Fig. 5(a)). To understand the mechanism of activation, the anode was autopsied to quantify the physico-chemical characteristics of the encapsulating mortar. Samples of the encapsulating mortar were collected from three Reference Regions (RR) 1, 2, and 3 (see Fig. 5(b)). Microanalytical tests were conducted to evaluate the characteristics of the encapsulating mortar, which are presented next.

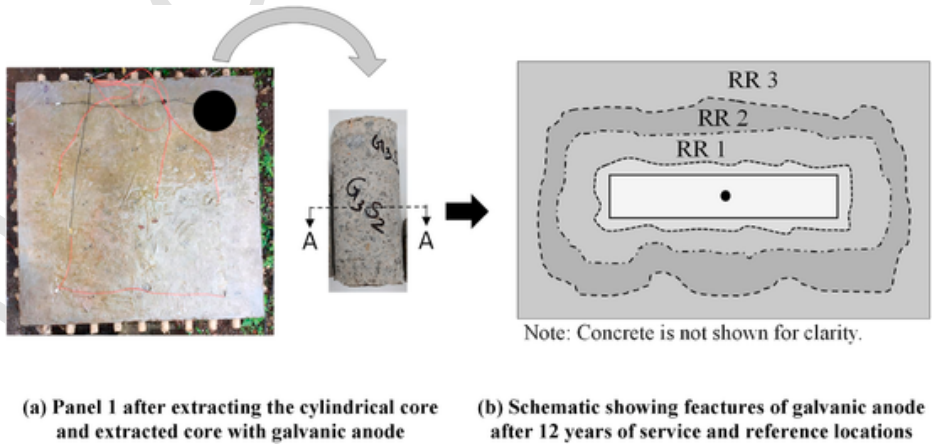

Fig. 5. Procedure followed to extract the anode from Part A1 of Panel 1. (a) Panel 1 after extracting the cylindrical core and extracted core with galvanic anode (b) Schematic showing features of galvanic anode after 12 years of service and reference locations.

3.2.1. Pore structure of encapsulating mortar

The porosity and critical pore sizes of the encapsulating mortar from RR1 and RR3 were determined using Mercury Intrusion Porosimetry (MIP) technique. The pore structure of mortar from RR2 was not analyzed due to insufficient sample size, which was used for determining the chemical composition. In this experimental program, Pascal 140–440® MIP instrument was used to measure the pore size in the range of 100 μm to 3 nm. Three fragments from the encapsulating mortar were collected from RR 1 and RR 3 with a total weight of about 0.3 g and thickness of each chunk ≈5 mm. These were used for the tests. Mercury was intruded inside the pores of the chunk and the total volume of mercury intruded was used to estimate the total porosity of the mortar samples. The critical pore entry diameter was the peak of the differential curve of the total volume of mercury intruded.

3.2.2. Chemical composition and pH of encapsulating mortar

The chemical composition of the encapsulating mortar from a virgin anode and an anode after 12 years of service from location RR 2 were evaluated using Energy Dispersive X-ray (EDX) Analysis. EDX analysis was selected because of the limitation of encapsulating mortar samples obtained from the anode. In addition, acid-base titrations were performed on the samples to calculate the residual lithium content and the approximate pH of encapsulating mortar in RR 1 and RR 3. For this, encapsulating mortar from the respective regions were ground to particle size less than 100 μm. Then, approximately 2 g of ground encapsulating mortar was mixed with 10 ml of de-ionized water and titrated against 1 mol/l Hydrochloric acid. The nominal pH of the solution was measured using a pH electrode. A titration curve between the amount of acid added and the nominal pH of solution was generated as per [19]. The amount of acid required to neutralize the hydroxyl buffer in the encapsulating mortar was calculated from the inflection point of the acid-base titration curves. This value was used to calculate the approximate amount of lithium hydroxide monohydrate ($LiOH.H_2O$.) in the mortar sample (termed as M1) as shown in Equation (4).

$$M1 = \frac{Volume\ of\ acid\ added \times Molecular\ weight\ of\ LiOH.H_2O}{1000} \quad (5)$$

Then, the mass of lithium hydroxide as a percentage of the dried sample mass (termed as M2) was calculated using Equation (5)

$$M2 = \frac{M1}{Dry\ weight\ of\ the\ sample} \times 100 \quad (6)$$

The mass of $LiOH.H_2O$ in the sample per 1000 ml of water (termed as M3) was calculated using Equation (6)

$$M3 = \frac{M2}{Evaporable\ water\ content\ of\ the\ sample} \times 100 \quad (7)$$

To determine the evaporable water content, the encapsulating mortar from location of interest was grounded and weighed (w1). Then, this sample was placed in the oven at a temperature of 105-110 °C for 24 h. Then, it was placed in deciccator until it cools, then weighed again (w2). The difference in weight (w1-w2) is the evaporable water content of the sample. The mass of 1 mol of $LiOH.H_2O$ is 42. The approximate pH of the mortar samples was determined using Equation (7)

$$Approximate\ pH = \log\left(\frac{M3}{42}\right) + 14 \quad (8)$$

After that, the encapsulating mortar was scrapped off from anode metal and the remaining piece was dissected into four quadrants to assess the condition of the zinc and the tie-wires.

4. Results and discussions

4.1. Phase I: Long-term exposure and electrochemical measurements of panel specimens

4.1.1. Depolarized corrosion potentials

Fig. 6 shows the 24-h depolarized corrosion potentials ($E_{24\text{-}h}$) of rebars in Panel 1 and the free corrosion potential of rebars in Panel 2 with reference to saturated calomel electrode (SCE). Note that all the rebars are interconnected when $E_{24\text{-}h}$ or free corrosion potentials are measured. The depolarized corrosion potentials were measured from 9 years after installation of anodes until 12 years, a period that consisted of severe environmental conditions. During this time, the average $E_{24\text{-}h}$ of the rebars in Panel 1 were found to be more positive than −270 mV_{SCE}. This indicates that the galvanic anodes have essentially protected the rebars from the admixed chlorides throughout the exposure period of 12 years. In addition, 48-h depolarized potentials were also measured. However, the depolarized potentials were within the range of typical scatter of half-cell potential measurements. Therefore, further depolarized potentials were not measured and anodes were connected again to the rebars. The depolarized potentials more positive than −270 mV_{SCE} is also justified by the output protection current, which is presented later in this paper.

On the other hand, at the end of 8 years, the free corrosion potentials of the rebars in Panel 2 were found to be more negative than −600 mV_{SCE}. Also, Panel 2 suffered from hairline cracks parallel to the rebars. This indicates that the rebars were corroding. Later, the crack width kept increasing due to radial pressure exerted by more corrosion products filling in the steel-concrete interface. At the end of 10 years, the crack width on the concrete surface was measured to be about 2 mm, which is significantly high. Also, measured corrosion potentials were more negative than −500 mV_{SCE} — indicating active corrosion.

4.1.2. Corrosion current density of steel rebar with and without galvanic anodes

Fig. 7 shows the average corrosion current density at the end of 10 years, which indicates the rate of corrosion. For the top rebars in depolarized conditions of Panel 1 the corrosion current density was found to be relatively insignificant (≈0.25 μA/cm²) and for the free corroding conditions of Panel 2 the corrosion current density was on average around 80 μA/cm². The insignificant corrosion rate of the rebars of Panel 1 clearly show that they were protected by the galvanic anodes. To the contrary, the rate of corrosion of the rebars of Panel 2 indicates that the rebars were experiencing severe corrosion in the same exposure environment as Panel 1. Therefore, the results on the

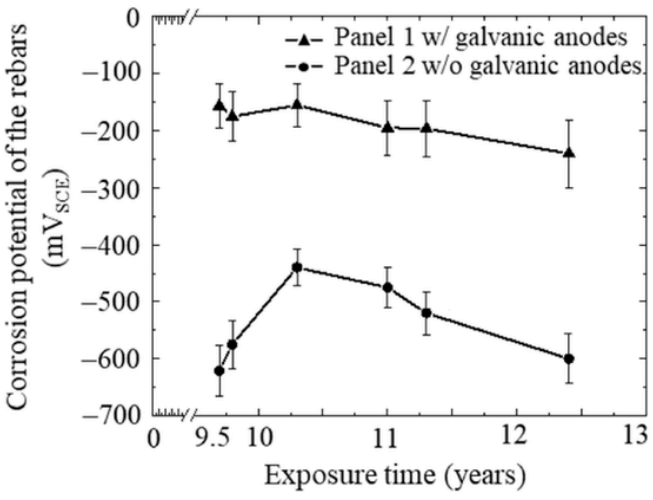

Fig. 6. Depolarized potential of rebars embedded in concrete panels.

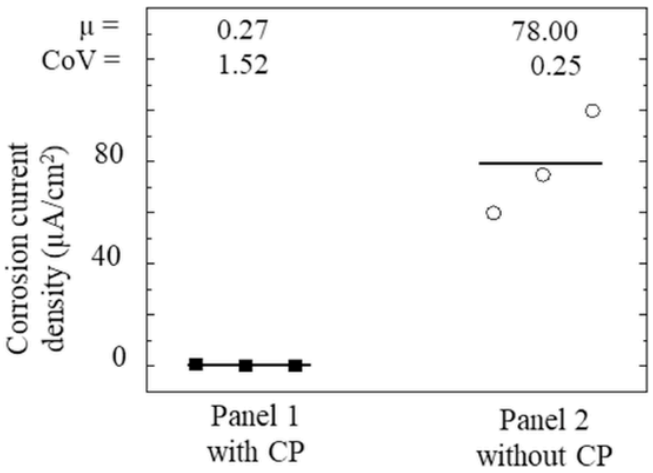

Fig. 7. Corrosion current density of the rebars at the end of 10 years after installation of anodes.

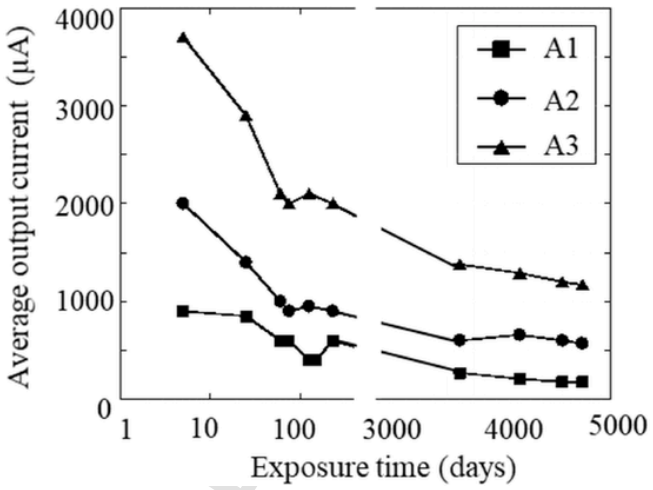

Fig. 8. Output current density from anodes showing that the anodes are in working condition even after 12 years or more.

rate of corrosion indicate that if the number and location of anodes are adequately designed, the rebars can be protected for the long term (say, more than 10 years). Number and location of anodes are designed based on the corrosion conditions of individual locations considering the rate of corrosion of rebars, chloride concentration in the concrete, electrical resistivity of the concrete in the location of interest, steel density, etc. Note that the rate of corrosion of the bottom rebars could not be measured due to the inaccessibility of the rebars.

The average corrosion current density of the rebars in Part A1, A2, and A3 of Panel 1 were found to be 0.75, 0.05, and 0.015 μA/cm^2. This indicates that the level of passivation of rebars were proportional to the surface area of the anode metal pieces i.e., A3 > A2 > A1. The influenced region of the panel from each anode was not estimated as it is out of the scope of this paper but a spacing of 400 mm was seen to have allowed adequate protection of all the steels. The corrosion current density of rebars in parts with A2 and A3 anodes were found to be less than 0.1 μA/cm^2, which shows that the rebars in parts with A2 and A3 were passivated as per NACE SP0290. However, the corrosion current density of one of the rebars in Part A1 was >0.1 μA/cm^2, which indicates that the anode connected in Part A1 to the rebar may not have sufficient surface area to supply the required protection current to passivate the whole length of the steel rebars. Therefore, the efficiency of anodes was evaluated by measuring the output current from anodes, which is discussed next.

4.1.3. Effect of surface area of anode metal on performance of galvanic anode

The rectangular, circular, and triangular markers in Fig. 8 show the average output current obtained from Anode sets A1, A2, and A3, respectively. The initial average output current from anodes of Type A1, A2, and A3 was about 900, 2,000, and 3700 μA, respectively. As expected, the output current density from the anodes was proportionally higher as the surface area increased. Note that the output currents were in the same ratio as the surface area of metal in the galvanic anodes (A1:A2:A3 = 1:2:4). As a consequence, anodes with the higher surface area were able to supply a higher current to the steel rebars. Therefore, the higher current output anodes will be expected to control the rate of corrosion of the steel sooner and easier than the anodes with the lower surface area. During initial exposure period (between 0 and 3 months), the output currents were found to be significantly decreasing. This can be attributed to following two factors: (i) the hydration of concrete – leading to maturity of concrete and increase in the resistivity of concrete and (ii) the surface of steel would have been active. Therefore, due to high demand and low electrolyte resistance the output currents were high. In about 2–3 months, the output current decreases exponentially for these types of anodes, then stabilised [23]. The significant decrease and stabilization of output current may also have been due to the build-up of the passivating oxide film on the surface of the steel rebars during their early protection and from the continued hydration of the concrete, which would have resulted in higher resistivity. The rate of decrease of output current was gradual from Year 1 to Year 12 (from about 200 days to 3700 days) after the installation of the anodes. Beyond the early rapid reduction, the current density is expected to be halved over constant time periods, which, for Anode A1, the aging factor (or half-life) appears to be 8.5 years. For Anodes A2 and A3, the aging factor appears to at least 13 years. The average surface electrical resistivity of concrete at 10- and 12-year age was found to be ˜ 17 kΩ?cm with coefficient of variation of 0.21. This timescale of halving of the current output was termed the 'Aging Factor' elsewhere [19,48]. Note that the duration during early rapid reduction of output current should be eliminated for calculation of Aging factor.

4.1.4. Visual inspection of panels after 12 years of natural exposure

Visual inspection, depicted in Fig. 9(a) shows that Panel 1 did not crack after 12 years of exposure to warm and humid environment even though it contained high chloride levels. The black lines in the photograph of Panel 1 are the wires used for electrical connection between the various anode and the rebars. The absence of cracks indicates that the anodes had successfully protected the steel from rebar corrosion even though the current density decreased with time. To identify why the current output had reduced with time, some microanalytical studies were conducted, which are discussed later. As shown in Fig. 9(b), Panel 2 suffered from significant cracking (see black lines drawn parallel to the crack on concrete). Fig. 9(b) shows the closeup of the top view of the crack on Panel 2 of the concrete surface – indicating that unprotected reinforced concrete structures with chloride contamination can undergo significant corrosion, cracking, spalling, and damage.

4.2. Phase II: Physico-chemical characteristics

4.2.1. Visual observation of the autopsied galvanic anode

Fig. 10(a) shows the curved surface area of the cylindrical concrete core extracted from Part A1 of Panel 1. A part of the anode was cut during coring as the precise location of the anode was not known. As expected, the unreacted zinc metal was found to be surrounded by a layer of white zinc corrosion products (zinc oxides/hydroxides). Also, it was observed that the zinc corrosion products had penetrated radially outwards into the encapsulating mortar until about half of the width surrounding the zinc metal piece. The porous encapsulating mortar could

Fig. 9. Photograph showing the condition of the panels after 12 years of exposure. Panel 2 shows severe corrosion (a) Panel 1 (with CP system) (b) Panel 2 (without CP system) and closeup of crack in Panel 2.

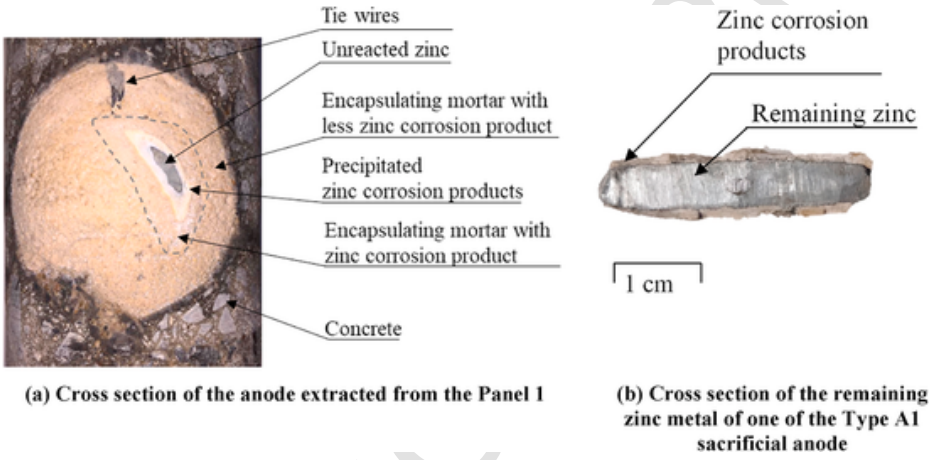

Fig. 10. Condition of the galvanic anode after 12 years (the encapsulating mortar is scraped off exposing the bare metal). (a) Cross section of the anode extracted from the Panel 1 (b) Cross section of the remaining zinc metal of one of the Type A1 sacrificial anode.

provide a path and facilitate the movement of corrosion products away from zinc metal — exposing the unreacted zinc surface and providing the contact of zinc metal to the encapsulating mortar with high pH, which is discussed later. Fig. 10(b) shows a cross-section of the unreacted zinc metal piece surrounded with yellow, dense, insoluble zinc corrosion products. In the absence of adequate moisture or relative humidity, zinc corrosion products can be highly resistive and interrupt the ionic conduction, which may result in premature failure of galvanic anodes. Approximately 1/4th of the thickness of zinc metal was found to be consumed in about 12 years of service – indicating that if the electrical connections and corrosive environment for the galvanic anode is adequate, the anode could protect the steel in Panel 1 for several more years, which will depend on the characteristics of encapsulating mortar and electrical connection between tie wires & zinc metal. Similarly, Dugarte and Sagüés [49] reported that the anodes stop functioning due to encapsulating mortar surrounding to galvanic metals failing to provide the adequate environment for continuous corrosion after about 1/4th of the galvanic metal is consumed. Note that the anode used for this investigation was extracted from the corner of the specimen, where it supplied current to less surface area of steel than other anodes (say, those more in the middle). Therefore, the investigated anode may be less consumed than other anodes. However, the rate of corrosion of depolarized steels and output current density from anodes showed that the anodes are still functioning. The anticipated performance of anodes in present study is discussed later based on the characteristics encapsulating mortar, tie wires, and electrical connection between tie wires and zinc metal.

4.2.2. Critical pore size and porosity

Fig. 11 shows that the $d_{critical}$ for the encapsulating mortars from RR 1 and RR 3 was found to be 0.1 and 1 μm, respectively. $d_{critical}$ is the maximum pore diameter that can connect the largest interconnected pores. It was found that $d_{critical}$ at RR 1 was about 10 times less than $d_{critical}$ of the mortar from RR 3 – indicating that a large volume of pores in RR 1 may have been filled with in-soluble zinc corrosion products. Porosity is defined as the ratio of the volume of pores in the encapsulating mortar sample to the total volume of the sample. The design porosity of the encapsulating mortar is ≈ 20%. The remaining porosity in RR1 and RR3 were ≈2% and 8%, which is ˜ 90% and 60% less than the designed porosity. The porosity of RR1 was ≈4 times lesser than the porosity of the encapsulating mortar in RR 3. The difference in the reduction of porosity can be due to the accumulation of the insoluble zinc corrosion products precipitating in the pore spaces. The zinc corrosion products get precipitated hence they build up more strongly close to the zinc metal. Therefore, if an adequate porosity is not provided in the encapsulating mortars, it can lead to clogging of the pore and can result in the deactivation of zinc metals due to reduced alkalinity in the vicinity of the zinc metal. In alkali activated galvanic anodes such as these ones, soluble zincate corrosion products are produced according to Equations (8) and (9). Their solubility allows them to move into the pores of the encapsulating mortar where they precipitate out as zinc ox-

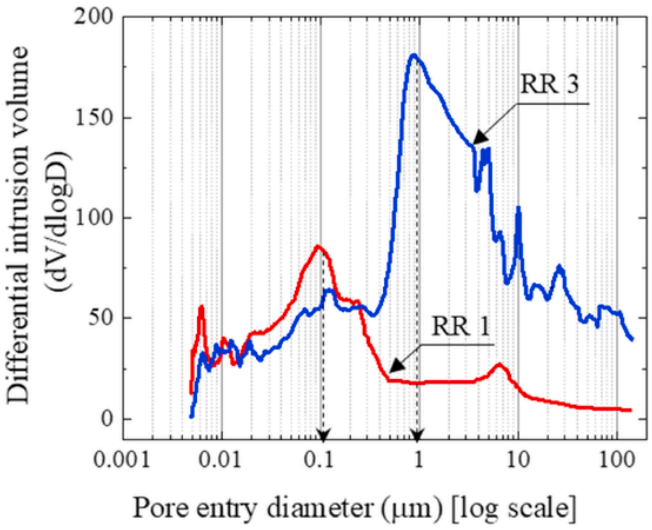

Fig. 11. Pore structure of the activating mortar at RR 1 and 3 determined using Mercury Intrusion Porosimetry (each curve is the average of three samples).

ide once supersaturation occurs. It is important, therefore, that enough porosity is present in the encapsulating mortar to allow percolation of the soluble corrosion products and avoid excessive blockage just at the zinc/mortar interface.

$$Zn + 2OH- \rightarrow Zn(OH)_2 + 2e^- \quad (9)$$

$$Zn(OH)_2 + 2OH^- \rightarrow Zn(OH)_4^{2-} \quad (10)$$

4.2.3. Chemical composition of the activating mortar and residual pH

Table 2 shows the chemical composition of the encapsulating mortar collected from the virgin anode and from RR 2 of the anode extracted from the Panel after 12 years of service. Elements like Mg, Al, Si, and Ca were found during the investigation. – Compounds of these elements might have been added to facilitate the encapsulating mortar with following (i) high ion exchange and (ii) long-term corrosive environment to prevent the passivation of the zinc. For example, calcium chloride, potassium acetate, potassium hydroxide, bentonite, and gypsum are used as humectants to maintain the humidity level in the galvanic anode [30,50,51]. Lithium hydroxide was used as activator [52]. Here, the total concentration of elements (Mg, Al, Si, Ca, Zn, O, K, and Fe) in encapsulating mortar from virgin anode was found to be about 75%. The remaining would have been Li concentration, which could not be detected because the atomic weight of Li is 6.9 g/mol, which is less than C (12.0 g/mol), which is the lightest element that can be determined by the instrument. On the other hand, the concentration of these elements in encapsulating mortar from anode after 12 years of service was found to be 100% - indicating that Lithium hydroxide get consumed and lithium migrates out of encapsulating mortar during the process to provide alkaline environment to the zinc metal. Simultaneously, the concentration of chlorides was found to increase from 0 to 3.78% due to migration from concrete to encapsulating mortar. The concentration of a few of the elements such as Mg, Al, and Si were found to be increasing (from-to) 0.26–4.52, 6.31–16.33, and 2.37–18.86, respectively. The concentration seemed to increase, which is misleading as the lithium has migrated out and the powder used does not contain Li. The concentration of LiOH was determined using the titration method, which is presented later.

Table 2
Chemical composition of encapsulating mortar at RR 2.

Element	Weight (%)	
	Virgin galvanic anode	Galvanic anode post 12 year of service
Mg	0.26	4.52
Al	6.31	16.33
Si	2.37	18.86
Cl	0.0	3.78
Ca	12.59	11.91
Zn	1.75	0.69
O	50.69	43.91
K	0.34	0
Fe	0.3	0
Li	Could not be detected using EDX.	

After 12 years of service, traces of chlorides were found in the encapsulating mortar. The presence of chlorides might be due to the diffusion or electromigration of the chloride ions from the contaminated concrete through the encapsulating mortar towards the electrochemically positive anode metal. The concentration of zinc was also found less than that of the virgin anodes. This can be attributed to dissolution of zinc corrosion products and their migration away from the zinc metal in the encapsulating mortar. In other words, availability of zinc in virgin encapsulating mortar was present in the encapsulating mortar (in region RR2) due to contamination during the manufacturing process. During the cathodic protection process, the anions produced at the cathodic sites (say, OH^-) may migrate towards the zinc metal. During this migration, they might react with the zinc to from soluble zincate. Then, these zincate ions may have got diffused outwards away from RR2. This process continues till the supersaturation state is achieved. This exchange of ions can alter the functionality of galvanic anodes. For example, if zinc corrosion products get filled in the pores of the encapsulating mortar at the zinc-encapsulating mortar interface, then the fresh zinc metal will not be adequately exposed to the activating materials in the encapsulating mortar. Also, due to filling of pores, the availability of humectants at the zinc metal surface can get reduced – leading to difficulty in maintaining a high humid micro-climate at zinc-encapsulating mortar interface, which can reduce the rate of corrosion of zinc. Also, the concentration of lithium was found to be decreasing from the location close of anode metal, which is presented next. Such alteration in characteristics of the anode can reduce the efficiency of galvanic anodes.

The acid-base titration curve was used to determine the approximate pH buffer of the encapsulating mortar in one of the samples. The approximate amount of LiOH and the pH buffer was calculated by using Equations (2)–(5). The solubility of $LiOH.H_2O$ in water at 20 °C is approximately 22.0 g/100 cc of water [53]. The value of $LiOH.H_2O$ determined at the RR 2 and RR 3 was found to be 17 and 22 g per 100 ml of water, which is more than the solubility of $LiOH.H_2O$ (220 g/l of water). This indicates that there is an excess LiOH in the samples, which will buffer the solution at a calculated pH of about 14.4. The value of $LiOH.H_2O$ determined at the RR 1 was found to be ≈ 1 g per 100 ml of water – indicating the reduction in the concentration of LiOH due to the reduced alkalinity of the mortar around the anode metal. The approximately calculated pH at this region was determined using Equation (5).

Fig. 12 shows that the calculated pH of encapsulating mortar in RR 1, 2, and 3 were found to be 14.1, 14.4, and 14.4, respectively. At Region 2 and 3, the concentration of LiOH was found to be greater than 220 g/l of water, indicating that there is excess LiOH in the sample which will buffer the solution at around pH 14.4. Therefore, the decrease in the pH buffer at RR1 can be due to the consumption of OH^- locally and electromigration of Li^+ away from the zinc, eventually reducing the level of LiOH to below saturation. However, the decrease in pH from 14.4 to 14 after 12 years of service may not be large enough to significantly alter the functionality of the galvanic anode. This continued good performance of the anodes can be attributed to the high pH and adequate porosity of the encapsulating mortar, which can maintain activity of the zinc metal and provide the path for the diffusion of soluble corrosion products away from the interface.

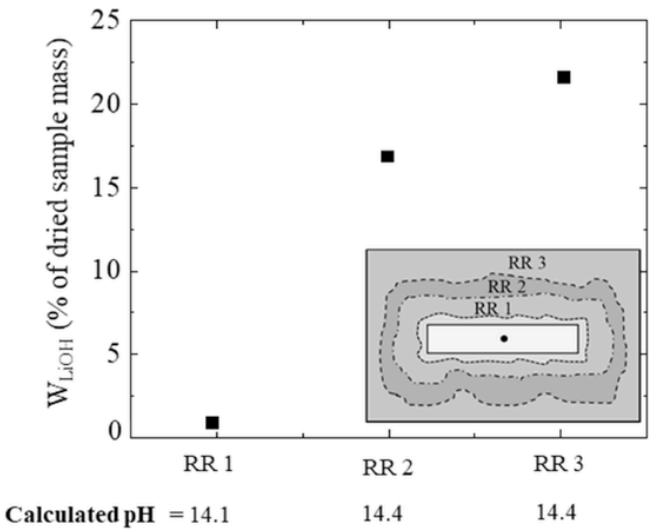

Fig. 12. Residual pH and lithium hydroxide content of the encapsulating mortar in Reference Regions 1, 2, and 3.

4.2.4. Electrical connection between zinc metal, tie wire, and rebars

Fig. 13 shows the photograph of the interface of the autopsied galvanic anode and tie wires. Fig. 13(a) shows that a layer of adherent insoluble zinc corrosion product was formed surrounding to the zinc metal surface. The corrosion products of zinc occupy the space vacated by the zinc metal and a part of it diffuses or migrates into the encapsulating mortar. In absence of moisture, the adherent semi-conductive zinc oxide layer can act as an increased barrier to the ionic conduction process [27,54], thereby decreasing the efficiency of the galvanic anodes in supplying electrons. Also, Fig. 13(a) shows the fractured surface of the anode metal piece. The tie wires had zinc corrosion products surrounding them, with a very small region left with an electrical connection to the zinc metal. Fig. 13(b) shows the fractured cross-section of zinc metal without the tie wires, where zinc corrosion product (white in color) are visible. Fig. 13(c) shows that the two tie wires were die cast at the time of manufacturing. The use of two tie wires close together may allow a space between them where molten zinc cannot penetrate. During the service life of anodes, moisture may enter into this space. Therefore, a galvanic cell can form between the zinc and tie wires. In this case and generally, tie wires are made of more electropositive metal than galvanic metal. Therefore, the zinc can corrode and form a layer of corrosion product surrounding the tie wire. In the rare event, this zinc oxide layer can completely cover the tie wires embedded in anode metal (zinc). Then, electric connection between the zinc core and the tie wires may be lost. Zinc oxide, being a semiconductor, will become more conductive in the presence of moisture and allow the flow of current [54,55]. Therefore, without moisture at the interface, the galvanic anode may not adequately protect the structure if the electrical connection between the zinc metal and tie wires is lost. With this learning, diecasting the zinc metal or zinc alloy on a single tie wire or well separated tie wires are recommended.

In addition, the material of tie wire can also affect the long-term performance of galvanic anodes. For example, mild steel tie wires can undergo surface corrosion during transportation and storage of galvanic anodes. Also, at repair sites, mild steel tie wires are tied to the steel rebars and left tied to steel rebars until the repair concrete is placed. During this time, the tie wires undergo surface corrosion [56]. At the time of installation, the electrical contact between the steel reinforcement and the tie wires (through the surfaces) should be ensured. At the time of installation, the rust from the tie wires will get exfoliated due to the abrasion, tying, and twisting processes. Therefore, it would get sufficient contact for electronic conduction. After that, both tie wires and steel rebars gets cathodically protected. If galvanic anodes are not installed with abrasion, tying, and twisting processes, the rust layer on tie wires of the galvanic anodes may hinder the supply of electrons to the steel rebars as expected. Considering this, galvanic anodes with corrosion-resistant metal tie wires (e.g., stainless steel) can be a good replacement for mild steel tie wires. Towards this, either the electrical connections should be checked just before placing the concrete or tie wires made of corrosion-resistant materials (say, stainless steel tie wires) should be used [57]. In short, anodes with corrosion-resistant, well-separated tie wires or anodes with corrosion-resistant single tie wire should be selected for cathodic protection.

4.2.5. Proposed mechanism of degradation of galvanic anode systems

Fig. 14 shows a possible degradation mechanism of galvanic anodes. Fig. 14(a) shows a virgin galvanic anode consisting of uncorroded zinc metal, two closely placed tie wires, and encapsulating mortar with interconnected pores. After several years of service and corrosion of the zinc metal, Fig. 14(b) shows that some of the zinc corrosion products can diffuse or migrate into the interconnected pore structure of the encapsulating mortar, and some corrosion products will simply fill the space vacated by the corroding zinc metal (see the zoomed image in Fig. 14(b)). The movement of the zinc corrosion product exposes the fresh zinc metal surface to the high pH of encapsulating mortar – helping to ensure the continued corrosion of zinc metal. If the porosity and interconnectivity of pores is not sufficient to expose the zinc metal, the effectiveness of the anode may decrease due to reduced ionic conductivity between zinc metal and the corroding rebars. In addition, the gap between two tie wires and between tie wire and

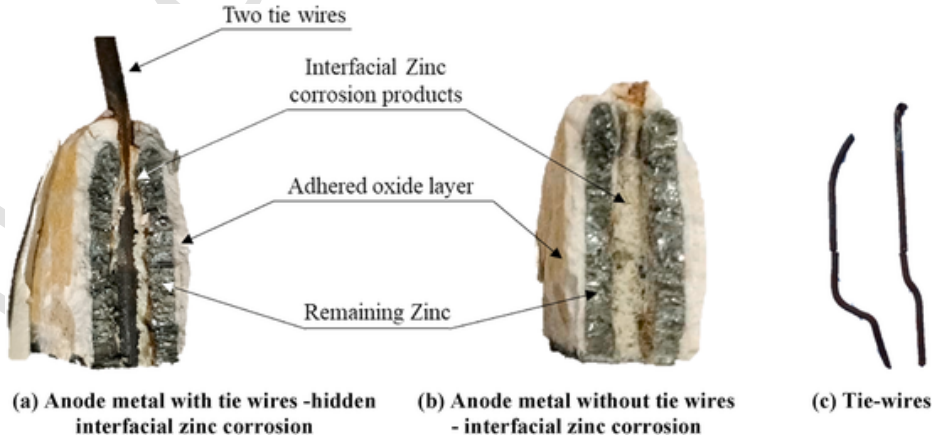

Fig. 13. Condition of anode metal (zinc) at the end of 12 years. (a) Anode metal with tie wires -hidden interfacial zinc corrosion (b) Anode metal without tie wires - interfacial zinc corrosion (c) Tie-wires.

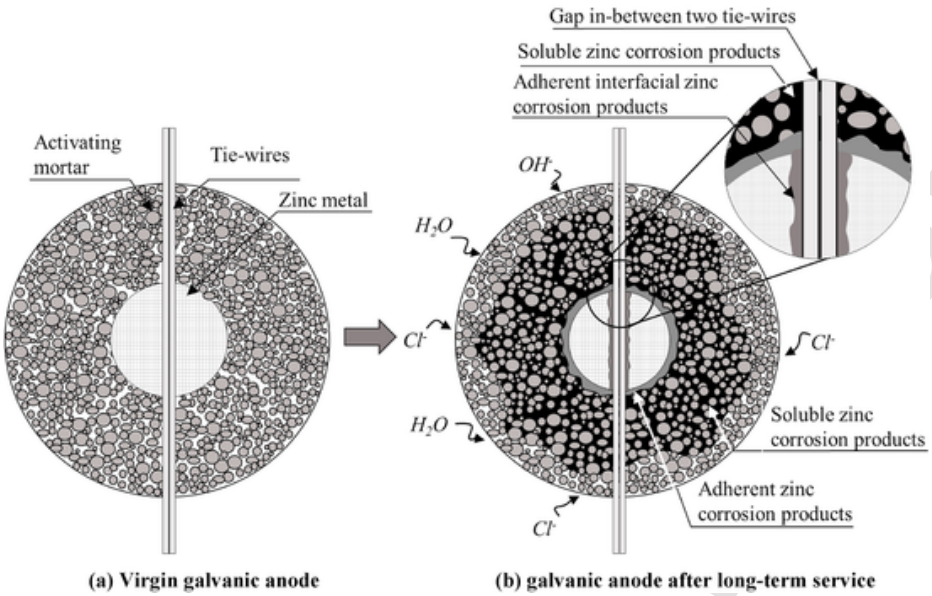

Fig. 14. Schematic showing the physico-chemical interactions in the encapsulating mortar. (a) Virgin galvanic anode (b) galvanic anode after long-term service.

the zinc metal may allow moisture to enter and result in interfacial corrosion of zinc metal (see the zoomed image in Fig. 14(b)). Once the corrosion products cover the tie wires and no moisture is available to provide electrical connection between them, the galvanic anode activity may decrease [54,55].

5. Recommendations for design of galvanic anodes

Based on the 12-year long performance assessment of the galvanic anodes and microanalytical studies on the galvanic anode, following are the recommendations to design durable for design of galvanic anodes in RC systems:

- Mass of the galvanic anode metals alone does not define their efficiency. The mass of galvanic anode metals can define how long the galvanic anodes can deliver current to the steel rebars, but the level of current will be governed by the design surface area of galvanic anode metals. Therefore, specifications should include considering both surface area of galvanic anode metals and the mass of the galvanic anode metals. The most important consideration is that sufficient current is provided over the design service life of the anode. Therefore, specifications considering the ratio of mass of galvanic anode metal (g) to the surface area of galvanic anode metal (cm^2) with minimum mass of anode metal can be introduced as one of the specifications. However, more research is required to propose an adequate ratio of mass and surface area of anode. However, the long-term level of current can be determined by knowledge of the 'Aging Factor' of the anode which defines the number of years required for the current output of the individual anode to be halved.
- An elevated pH of the encapsulating mortar keeps the galvanic metal active. In another publication [19], the output current from the galvanic anode was found to reduce when the pH of encapsulating mortar was less than 13.8. In this research, the pH at zinc-encapsulating interface was found to be 14.1, which can still help the zinc to corrode. Considering results from Ref. [19], the concentration of the activator should be chosen such that the pH of encapsulating mortar is > 13.8 and preferably >14 throughout the service life of galvanic anode.
- The pore structure in combination with the high pH environment which allows the zincate corrosion products to remain soluble, helps to accommodate the corrosion products of the galvanic metal. Therefore, minimum porosity of the encapsulating mortar should be designed and, according to recent estimates, should be >20% of volume of encapsulating mortar (≈200 mm^3/g). In this research, it was found that the adequate diffusion or migration of corrosion products was possible when the encapsulating mortar have the critical pore size ($d_{critical}$) in the range of 5–15 μm. A higher $d_{critical}$ may be an advantage as the current output was seen to diminish with time, but more work is required to establish $d_{critical}$ and total pore volume of the encapsulating mortar.
- To avoid formation of a rust layer on the tie wires during transportation, storage, and placement, corrosion-resistant materials such as stainless steel should be used for tie wires.
- To avoid corrosion at the interface of adjacent embedded lengths of the tie wires and the galvanic anode metal, the anode metal should be diecast around well-separated (say, at least 0.5 mm apart) corrosion-resistant tie-wires or a single tie wire. Furthermore, the tie-wires should not be attached to the anode metal either by welding or other means.
- The resistance between tie wire and the rebar onto which the anode is attached should not be more than 1 Ω. This should be established during the installation of the anode.

Table 3 summarizes the recommendations for the selection of galvanic anodes.

6. Summary and conclusions

The 12 year-long performance of galvanic anodes was assessed using two reinforced concrete panel specimens with and without anodes with 2% chloride ion by mass of binder added. For this, electrochemical measurements, such as depolarized corrosion potential, output current, and corrosion current density, were performed. The results indicate that the galvanic anodes were able to passivate the steel reinforcement even in highly aggressive warm and humid environments for about 12 years. With adequate design and intact electrical connections, the cathodic protection approach is expected to mitigate reinforcement corrosion in similar environments (concrete with chlorides) for about 10–15 years. This duration can be longer when adequately designed durable galvanic anodes are installed to rebars without corrosion or not sufficient chlorides in the vicinity of steel rebars. The output protection current has roughly halved between say Month 6 and Year 12, which indi-

Table 3
Proposed specifications of galvanic anodes.

Characteristic/parameter	Recommended specification
Maximum ratio of mass of galvanic anode metal (g) to the surface area of galvanic anode metal (cm^2)	To be decided based on aging factor, which can ensure to provide sufficient current is provided over the targeted service life of the anode.
Minimum calculated pH throughout the service life of galvanic anode	13.8
Minimum porosity of encapsulating mortar	20% of the total volume of encapsulating mortar
Critical pore size	Minimum 5 μm. To decide the upper limit, more research is required.
Material of tie wire	Stainless steel or similarly corrosion-resistant steel
Minimum distance between tie wires (if more than 1 tie wire is used)	0.5 mm
The connection between anode metal and tie wire(s)	Any method which can aggravate the corrosion is prohibited. For example, welding of tie wire and galvanic anode metal is not allowed Electrical connections between the anode metal and the steel reinforcement should be ensured until the full consumption of the galvanic anode metal.

cates that an 'Aging factor' may be determined, which can aid in the long-term design of the required current output.

After 12 years of service, microanalytical studies such as pore size distribution, localized pH determinations, and chemical composition analysis of the encapsulating mortar at various locations were conducted to understand the degradation mechanisms of the anodes. Note that the anode used in this investigation was extracted from the corner of the specimen – indicating that the investigated anode may be less consumed than other anodes. The critical pore size ($d_{critical}$) in encapsulating mortar near (RR1) and away (RR3) from the anode metal was found to be 1 and 10 μm. Similarly, the remaining porosity in RR1 and RR3 were ≈90% and 60% less than the designed porosity, respectively. The reduction in $d_{critical}$ and porosity of encapsulating mortar indicate that the zinc corrosion products diffuse/migrate away from the anode metal. Therefore, adequate $d_{critical}$ can facilitate the long-term performance of galvanic anodes. Further research is required to understand how the reduction in pore size will affect the conductivity of encapsulating mortar. In addition, the interface corrosion of tie wire and zinc metal highlights the importance of diecasting with gap between tie wires and between tie wire and galvanic anode filled with galvanic anode metal. Based on these, specifications are proposed to design the galvanic anodes to achieve the durable service life.

Author statement

1. Deepak K. Kamde: Conceptualization, Methodology, Investigation, Formal Analysis, Visualization, Writing - original draft 2. Karthikeyan Manickam: Investigation, Formal analysis, and Writing - Review & Editing 3. Radhakrishna G. Pillai: Conceptualization, Writing - Review & Editing, Visualization, and Funding acquisition 4. George Sergi: Conceptualization, Writing - Review & Editing, Visualization, and Resources.

Declaration of competing interest

The authors declare that they have no known competing financial interests or personal relationships that could have appeared to influence the work reported in this paper.

Acknowledgements

The authors acknowledge the financial support (Project No. EMR/2016/003196) received from the Science and Engineering Research Board, Department of Science and Technology and the partial financial support from the Ministry of Human Resource Development of the Government of India. We thank Mr. Dhruvesh Shah for his help in storing the Panels. We thank Dr. Prakash Nanthagopalan and the staff at the Department of Civil Engineering, IIT Bombay for providing the laboratory space and support during testing.

References

[1] L. Bertolini, E. Redaelli, Depassivation of steel reinforcement in case of pitting corrosion: detection techniques for laboratory studies, Mater. Corros. Und Korrosion. 60 (2009) 608–616, https://doi.org/10.1002/maco.200905276.
[2] R.B. Polder, G. Leegwater, D. Worm, W. Courage, Service life and life cycle cost modelling of cathodic protection systems for concrete structures, Cement Concr. Compos. 47 (2013) 69–74, https://doi.org/10.1016/j.cemconcomp.2013.05.004.
[3] D. Kamde, R. Pillai, Effect of Sunlight/ultraviolet Exposure on the Corrosion of Fusion Bonded-Epoxy (FBE) Coated Steel Rebars in Concrete, CORROSION, 2020, https://doi.org/10.5006/3588.
[4] D.K. Kamde, R.G. Pillai, Effect of surface preparation on corrosion of steel rebars coated with cement-polymer-composites (CPC) and embedded in concrete, Construct. Build. Mater. 237 (2020) 1–11, https://doi.org/10.1016/j.conbuildmat.2019.117616.
[5] G. Koch, J. Varney, N. Thompson, O. Moghissi, M. Gould, J. Payer, International Measures of Prevention , Application , and Economics of Corrosion Technologies Study, 2016 http://impact.nace.org/documents/Nace-International-Report.pdf.
[6] G.P. Tilly, J. Jacob, Concrete Repairs - Performance in Service and Current Practice, EN 1504 Se, IHS BRE Press, Bracknell, 2007.
[7] N. Krishnan, D.K. Kamde, Z.D. Veedu, R.G. Pillai, D. Shah, V. Rajendran, Long-term performance and life-cycle-cost benefits of cathodic protection of concrete structures using galvanic anodes, J. Build. Eng. (2021) In press.
[8] G. Sergi, Ten-year results of galvanic sacrificial anodes in steel reinforced concrete, Mater. Corros. 62 (2011) 98–104, https://doi.org/10.1002/maco.201005707.
[9] C. Christodoulou, C. Goodier, S. Austin, J. Webb, G.K. Glass, Diagnosing the cause of incipient anodes in repaired reinforced concrete structures, Corrosion Sci. 69 (2013) 123–129, https://doi.org/10.1016/j.corsci.2012.11.032.
[10] C. Christodoulou, C.I. Goodier, S.A. Austin, G.K. Glass, J. Webb, A new arrangement of galvanic anodes for the repair of reinforced concrete structures, Construct. Build. Mater. 50 (2014) 300–307, https://doi.org/10.1016/j.conbuildmat.2013.09.062.
[11] M.O. Kim, A. Bordelon, M.K. Lee, B.H. Oh, Cracking and failure of patch repairs in RC members subjected to bar corrosion, Construct. Build. Mater. 107 (2016) 255–263, https://doi.org/10.1016/j.conbuildmat.2016.01.017.
[12] R.B. Polder, W.H.A. Peelen, W.M.G. Courage, Non-traditional assessment and maintenance methods for aging concrete structures - technical and non-technical issues, Mater. Corros. 63 (2012) 1147–1153, https://doi.org/10.1002/maco.201206725.
[13] K. Wilson, M. Jawed, V. Ngala, The selection and use of cathodic protection systems for the repair of reinforced concrete structures, Construct. Build. Mater. 39 (2013) 19–25, https://doi.org/10.1016/j.conbuildmat.2012.05.037.
[14] F. Sandron, D.W. Whitmore, P. Eng, Galvanic Protection for Reinforced Concrete Bridge Structures, 2005, pp. 1–14.
[15] L. Bertolini, M. Gastaldi, M.P. Pedeferri, E. Redaelli, Prevention of steel corrosion in concrete exposed to seawater with submerged sacrificial anodes, Corrosion Sci. 44 (2002) 1497–1513, https://doi.org/10.1016/S0010-938X(01)00168-8.
[16] E. Redaelli, F. Lollini, L. Bertolini, Throwing power of localised anodes for the cathodic protection of slender carbonated concrete elements in atmospheric conditions, Construct. Build. Mater. 39 (2013) 95–104, https://doi.org/10.1016/j.conbuildmat.2012.05.014.
[17] F.J. Presuel-Moreno, S.C. Kranc, A.A. Sagüés, Cathodic prevention distribution in partially submerged reinforced concrete, Corrosion 61 (2003) 548–558, https://doi.org/10.5006/1.3278190.
[18] L. Bertolini, E. Redaelli, Throwing power of cathodic prevention applied by means of sacrificial anodes to partially submerged marine reinforced concrete piles: results of numerical simulations, Corrosion Sci. 51 (2009) 2218–2230, https://doi.org/10.1016/j.corsci.2009.06.012.
[19] G. Sergi, G. Seneviratne, D. Simpson, Monitoring results of galvanic anodes in steel reinforced concrete over 20 years, Construct. Build. Mater. 269 (2021) 121309, https://doi.org/10.1016/j.conbuildmat.2020.121309.
[20] B.S. EN ISO 12696:2012, BSI Standards Publication Cathodic Protection of Steel in Concrete, BSI, Brussels, 2012 (ISO 12696 : 2012).
[21] A. Goyal, H. Sadeghi, E. Ganjian, A. Omotayo, Predicting the corrosion rate of steel in cathodically protected concrete using potential shift, Construct. Build. Mater. 194 (2019) 344–349, https://doi.org/10.1016/j.conbuildmat.2018.10.153.
[22] C. Christodoulou, G. Glass, J. Webb, V. Ngala, S. Beamish, P. Gilbert, Evaluation of Galvanic Technologies Available for Bridge Structures, 2008, pp. 10–12.
[23] J.C. Ball, D.W. Whitmore, Embedded galvanic anodes for targeted protection in reinforced concrete structures, Cocrete Repair Bull. 22 (2009) 6–9.
[24] O.T. De Rincón, A. Torres-Acosta, A. Sagüés, M. Martinez-Madrid, Galvanic anodes for reinforced concrete structures: a review, Corrosion 74 (2018) 715–723, https://

doi.org/10.5006/2613.
[25] D. Whitmore, M. Miltenberger, Galvanic cathodic protection of corroded reinforced concrete structures, NACE - Int. Corros. Conf. Ser. (2019) 2019-March.
[26] R. Polder, W. Peelen, Cathodic protection of steel in concrete-experience and overview of 30 years application, MATEC Web Conf., Int. Conf. Concr. Repair, Rehabil. Retrofit., 2018, p. 6, https://doi.org/10.1051/matecconf/201819901002.
[27] W. Schwarz, M. Bakalli, M. Donadio, A novel type of discrete galvanic zinc anodes for the prevention of incipient anodes induced by patch repair, Eur. Corros. Congr. EUROCORR 2016 (2016) 2136–2144.
[28] I. Genesca, L. Betancourt, L. Jerade, C. Rodriguez, F.J. Rodriguez, Electrochemical testing of galvanic anodes, Mater. Sci. Forum 289–292 (1998) 1275–1288, https://doi.org/10.4028/www.scientific.net/msf.289-292.1275.
[29] M.J. Dugarte, A.A. Sagüés, Sacrificial point anodes for cathodic prevention of reinforcing steel in concrete repairs: Part 1-polarization behavior, Corrosion 70 (2014) 303–317, https://doi.org/10.5006/1016.
[30] D. Whitmore, S. Abbott, Using humectants to enhance the performance of embedded galvanic anodes, NACE - Int. Corros. Conf. Ser., NACE International, San Diego, 2003, pp. 1–9.
[31] N. Idusuyi, O. Oluwole, Aluminium anode activation research- a review, Int. J. Sci. Technol. 2 (2012) 561–565.
[32] N. Khomwan, P. Mungsantisuk, Startup Thailand: a new innovative sacrificial anode for reinforced concrete structures, Eng. J. 23 (2019) 235–261, https://doi.org/10.4186/ej.2019.23.4.235.
[33] G. Sergi, G. Seneviratne, Improved design consideration for steel reinforcement corrosion control with galvanic anodes following performance evaluation from analysis of site data, Struct. Faults Repair, 2021 Edinburgh.
[34] J. Genescà Ferrer, J. Juárez, Development and testing of galvanic anodes for cathodic protection, Contrib. Sci. (Los Angel.) 1 (2000) 331–343.
[35] G. Sergi, C.L. Page, Sacrificial anodes for cathodic prevention of reinforcing steel around patch repairs applied to chloride-contaminated concrete, Eurocorr 99 (1999) 1–9.
[36] W.J. Smith, F.E. Goodwin, Hot dip coatings, Ref. Modul. Mater. Sci. Mater. Eng. (2017) 1–19, https://doi.org/10.1016/b978-0-12-803581-8.09214-6.
[37] G.T. Parthiban, T. Parthiban, R. Ravi, V. Saraswathy, N. Palaniswamy, V. Sivan, Cathodic protection of steel in concrete using magnesium alloy anode, Corrosion Sci. 50 (2008) 3329–3335, https://doi.org/10.1016/j.corsci.2008.08.040.
[38] O.T. De Rincon, A.R. de Carruyo, D. Romero, E. Cuica, Evaluation of the effect of oxidation products of aluminum sacrificial anodes in reinforced concrete structures, Corrosion 48 (1992) 960–967, https://doi.org/10.5006/1.3315900.
[39] C. Christodoulou, C.I. Goodier, S.A. Austin, Site performance of galvanic anodes in concrete repairs, Concr. Solut. - Proc. Concr. Solut. 5th Int. Conf. Concr. Repair. (2014) 167–172, https://doi.org/10.1201/b17394-28.
[40] Weather Online, 2020 (accessed December 21, 2020) https://www.weatheronline.in/weather/maps/city.
[41] J.A. Gonzalez, M. Benito, S. Feliu, P. Rodriguez, C. Andrade, Suitability of assessment methods for identifying active and passive zones in reinforced concrete, Corrosion 51 (1995) 145–152, https://doi.org/10.5006/1.3293586.
[42] P.C. Andrade, C. Alonso, R. Polder, R. Cigna, O. Vennesland, M. Salta, A. Raharinaivo, B. Elsener, Rilem TC 154-EMC : ' Electrochemical Techniques for Measuring Metallic Corrosion ' Test methods for on-site corrosion rate measurement of steel reinforcement in concrete by means of the polarization resistance method, Mater. Struct. 37 (2004) 623–643.
[43] S. Feliu, J.A. González, C. Andrade, Multiple-electrode method for estimating the polarization resistance in large structures, J. Appl. Electrochem. 26 (1996) 305–309, https://doi.org/10.1007/BF00242100.
[44] H. Wojtas, Determination of corrosion rate of reinforcement with a modulated guard ring electrode; analysis of errors due to lateral current distribution, Corrosion Sci. 46 (2004) 1621–1632, https://doi.org/10.1016/j.corsci.2003.10.007.
[45] S. Laurens, P. Hénocq, N. Rouleau, F. Deby, E. Samson, J. Marchand, B. Bissonnette, Steady-state polarization response of chloride-induced macrocell corrosion systems in steel reinforced concrete - numerical and experimental investigations, Cement Concr. Res. 79 (2016) 272–290, https://doi.org/10.1016/j.cemconres.2015.09.021.
[46] U. Angst, M. Büchler, On the applicability of the Stern-Geary relationship to determine instantaneous corrosion rates in macro-cell corrosion, Mater. Corros. 66 (2015) 1017–1028, https://doi.org/10.1002/maco.201407997.
[47] U. Angst, M. Büchler, A new perspective on measuring the corrosion rate of localized corrosion, Mater. Corros. 71 (2020) 808–823, https://doi.org/10.1002/maco.201911467.
[48] D. Whitmore, G. Sergi, Long-term monitoring provides data required to predict performance and perform intelligent design of galvanic corrosion control systems for reinforced concrete structures, NACE Corros. Conf. Expo, 2021.
[49] M.J. Dugarte, A.A. Sagüés, Galvanic Point Anodes for Extending the Service Life of Patche Areas upon Reinforced Concrete Bridge, 2009.
[50] G.R. Holcomb, B.S. Covino, J.H. Russell, S.J. Bullard, S.D. Cramer, W.K. Collins, J.E. Bennett, H.M. Laylor, Corrosion 2000, 2000.
[51] J.E. Bennett, Activating Matrix for Cathodic Protection, US, 2009 2009/0183998 A1, https://doi.org/10.1016/j.ijpharm.2017.08.087%0A10.1016/j.ccr.2011.01.031.
[52] G.K. Glass, A.C. Roberts, N. Davison, Sacrificial Anode and True Treatment of Concrete, US, 2012 2012/0261270 A1.
[53] E.F. Stephan, P.D. Miller, Solubility of lithium hydroxide in water and vapor pressure of solutions above 220° F, J. Chem. Eng. Data 7 (1962) 501–505, https://doi.org/10.1021/je60015a018.
[54] G. Milano, M. Luebben, M. Laurenti, S. Porro, K. Bejtka, S. Bianco, U. Breuer, L. Boarino, I. Valov, C. Ricciardi, Ionic modulation of electrical conductivity of ZnO due to ambient moisture, Adv. Mater. Interfaces. 6 (2019) 1–9, https://doi.org/10.1002/admi.201900803.
[55] T.K. Roy, D. Sanyal, D. Bhowmick, A. Chakrabarti, Temperature dependent resistivity study on zinc oxide and the role of defects, Mater. Sci. Semicond. Process. 16 (2013) 332–336, https://doi.org/10.1016/j.mssp.2012.09.018.
[56] M. Natesan, G. Venkatachari, N. Palaniswamy, Kinetics of atmospheric corrosion of mild steel, zinc, galvanized iron and aluminium at 10 exposure stations in India, Corrosion Sci. 48 (2006) 3584–3608, https://doi.org/10.1016/j.corsci.2006.02.006.
[57] S.H. Mameno, R. Pettersson, C. Leygraf, L. Wegrelius, Atmospheric corrosion resistance of stainless steel: results of a field exposure program in the middle-east, Eur. Corros. Congr. EUROCORR 2 (2015) 1244–1254, https://doi.org/10.1007/s00501-016-0447-9.